Time-resolved fluorescence spectroscopy of two-photon laser-excited 8*p*, 9*p*, 5*f*, and 6*f* levels in neutral xenon

Christoph Eichhorn,[1,*] Stephan Fritzsche,[2,3] Stefan Löhle,[1] Andreas Knapp,[1] and Monika Auweter-Kurtz[4]
[1]*Institut für Raumfahrtsysteme, Universität Stuttgart, Pfaffenwaldring 31, D-70569 Stuttgart, Germany*
[2]*Gesellschaft für Schwerionenforschung (GSI), D-64291 Darmstadt, Germany*
[3]*Department of Physical Sciences, University of Oulu, P.O. Box 3000, Oulu Fin-90014, Finland*
[4]*Universität Hamburg, Edmund-Siemers Allee 1, D-20196 Hamburg, Germany*
(Received 14 April 2009; published 6 August 2009)

Laser-induced fluorescence of two-photon excited 8*p*, 9*p*, $J=0,2$ and 5*f*, 6*f*, $J=2$ levels in neutral xenon has been investigated in the pressure regime between 4 and 120 Pa. Radiative lifetimes and collisional deactivation rates have been deduced especially for the $5f[3/2]_2$, $5f[5/2]_2$, and $8p[1/2]_0$ levels using the Stern-Volmer approach. The spontaneous lifetimes for $5f[3/2]_2$, $5f[5/2]_2$, and $8p[1/2]_0$ levels are 94, 78, and 207 ns, respectively. These lifetimes have been calculated also by applying extended multiconfiguration Dirac-Fock wave functions and are found in agreement with experiment within 10–25 %.

DOI: 10.1103/PhysRevE.80.026401 PACS number(s): 52.38.−r, 32.80.Rm, 32.70.Cs

I. INTRODUCTION

Laser spectroscopic measurements are widely used for nonintrusive imaging of atoms and molecules in chemically reacting gas flows [1]. The advantage of laser-induced fluorescence techniques, in particular, is its high sensitivity of the fluorescence signal whereby quantitative results for different parameters such as local particle densities and temperatures are accessible. Even for plasma flows that occur with high speed and temperatures as typically for plasma wind tunnels in simulation of re-entry conditions for space vehicles, an estimation of the particle density of atoms is feasible. Thereby, the excitation of the atoms in the vacuum UV is usually achieved by spectroscopic approaches such as two-photon absorption laser-induced fluorescence (TALIF). In those re-entry simulation investigations, the focus lies on atomic oxygen and nitrogen measurements [2,3] due to its importance for the thermochemical interaction with heat shield materials.

Apart from these low-*Z* gases, xenon is of interest for applied plasma diagnostics. Xenon is used as propellant for electric in-space propulsion, where the research is currently focused on a realistic estimate of the particle number density in the plasma plume of ion thrusters. Moreover, the TALIF method requires particular calibration techniques in order to account for the nonlinear character of a two-photon excitation process. In recent publications, Goehlich *et al.* [4] and Niemi *et al.* [5,6] showed that measurements relative to xenon and krypton are a promising approach for calibrating the atomic oxygen and nitrogen TALIF measurements. In practice, there are numerous transitions for xenon which can be applied to this approach as well as for the electric propulsion plasma diagnostics. The quantitative investigation of a variety of TALIF schemes in xenon with respect to transition probabilities, as well as TALIF schemes in the spectral vicinity to two-photon resonances in other plasma species, is therefore important for their later application in plasma diagnostic experiments.

For any quantitative analysis of TALIF signals with respect to particle densities, however, the knowledge of the effective lifetimes and two-photon absorption cross sections is required. In the past, most experiments on the two-photon excitation of xenon concentrated on the measurement of radiative lifetimes of the levels from the 6*p* and 7*p* multiplets as well as on studying the state-to-state collision kinetics [7–12]. On the other hand, there is some lack of data with respect to two-photon absorption cross sections. Data are available for ground state excitation only involving 6*p* and one of the 7*p* levels [5,6,13–17]. While the two-photon excitation of higher excited levels, which belong to the 8*p* and 4*f* manifolds, has been already mentioned by Miller [18], his work was focused on the stimulated emission and the effects of multiphoton ionization. No two-photon excitation of the 5*f*, 6*f*, and 9*p* levels in atomic xenon has been reported so far in literature.

In the present investigation, TALIF spectroscopy is extended to levels of the 8*p*, 9*p*, 5*f*, and 6*f* manifolds with the perspective to utilize these levels for plasma diagnostic applications. In a first step, we therefore investigate the radiative and collisional transition rates. Up to the present, however, much less is known about these levels when compared with the 6*p* and 7*p* configurations. This applies especially for the spontaneous lifetimes and the collisional transition rates, as well as for the branching ratios. For the $5p^5nf$ ($n=4-8$) levels, in fact, there exists only one comprehensive study of the radiative lifetimes by Verdugo *et al.* [19]. These authors used electron-impact excitation in order to populate the excited levels. Some of these levels have been reinvestigated recently [20]. Moreover, lifetimes for some levels that belong to the 8*p* multiplet have been measured [21–24]. In our study, we did not measure new spontaneous lifetimes. The goal is rather to test the feasibility of these levels for TALIF spectroscopy. However, especially in the case of the 5*f* levels, lifetime measurements based on narrow band excitation are worthwhile since the only available data by Verdugo *et al.* [19] have been achieved using a much less state-selective excitation technique, and they did not resolve the fine structure completely in their analysis of the fluorescence signals.

*eichhorn@irs.uni-stuttgart.de

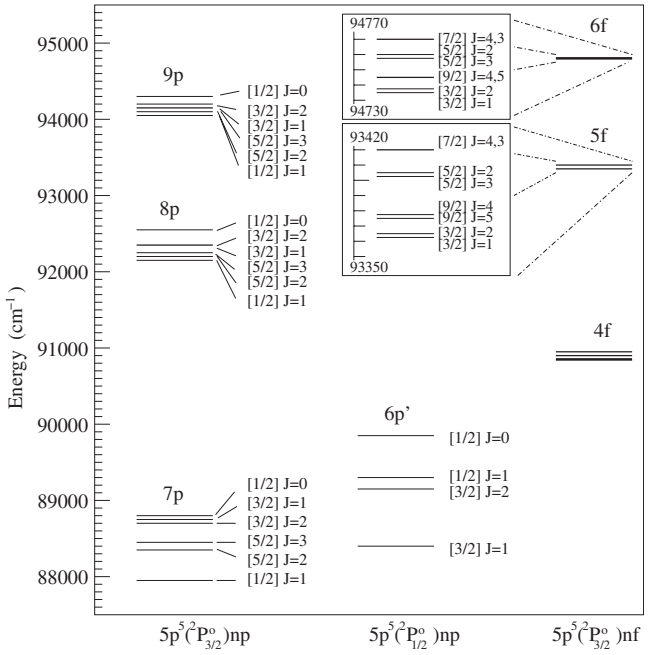

FIG. 1. Partial energy diagram of even parity states in neutral xenon. Levels are designated in Racah notation [25].

The electric-dipole selection rules for two-photon excitation require transitions between states of equal parity. In Fig. 1, we display a partial term diagram of neutral xenon, accounting for even parity levels. $5f$, $6f$ $J=2$ and $8p$, $9p$ $J=0,2$ levels are allowed to be populated via two-photon absorption from the ground state. In the following paragraphs, the widely used $nl[K]_J$ notation, which has been introduced by Racah [25], is used. In this notation, n and l designate the principal and the orbital angular momentum quantum numbers of the excited electron, respectively. The quantum number K corresponds to the total angular momentum of the core coupled to the orbital angular momentum of the excited electron, while J represents the total angular momentum, including the spin of the valence electron.

In this paper, we report about measurements of the lifetimes of some even parity levels in neutral xenon, excited by two-photon absorption. Detailed investigations have been carried out for the $5f[3/2]_2$, $5f[5/2]_2$, and $8p[1/2]_0$ levels. From the pressure-dependent measurements of the effective lifetimes the spontaneous lifetime is derived from a Stern-Volmer plot (lifetimes vs pressure). Energies and spontaneous lifetimes have been calculated also by using extended multiconfiguration Dirac-Fock (MCDF) computations. The measurements are an important prerequisite for the determination of two-photon absorption cross sections, which forms the basis to apply the TALIF technique for plasma diagnostics.

II. EXPERIMENT

Two-photon transitions in xenon atoms have been induced by applying a pulsed dye laser (Scanmate 2E, Lambda Physics), pumped with the third harmonic of a Nd:YAG laser (Quantel Brilliant B). The temporal full width at half maximum (FWHM) for the pulse is 4.9 ns. Laser pulses have been generated at a repetition rate of 10 Hz. The output of the dye laser is frequency doubled using a β-barium borate crystal. The spectral line shape of the dye laser has been checked and a FWHM linewidth of 0.1 cm^{-1} was found, which is narrow enough for a state-selective optical excitation of all fine-structure components of interest. Investigations have been performed by using Stilbene-3 as laser dye which enables to tune the laser frequency in the wavelength range between 2×207 and 2×220 nm. The wavelength can be adjusted in 0.5 pm steps for frequency-doubled photons. The laser beam has been focused by a lens system in a xenon filled static gas cell. Power densities at the detection volume have been varied between 5 and 30 MW/cm^2. Before the measurements were performed, the cell has been evacuated to a pressure of 10^{-5} Pa. For all investigations, 99.99% grade xenon has been utilized. The distance between the focal point and the lens system is 150 cm. Laser-induced fluorescence is collected by an achromatic lens with a focal width of 30 cm at a distance of 100 cm. These special geometrical dimensions allow for the later application of this setup for studying xenon plasmas in the plume ion thrusters, whose operation requires large-sized vacuum facilities.

Fluorescence signals are detected perpendicular to the direction of the laser beam by using a gated photomultiplier (Hamamatsu R636-10). This photomultiplier is sensitive for the detection of radiation in the range between 180 and 930 nm. For each level, excited by two-photon absorption, the fluorescence radiation was isolated by means of some appropriate narrow band interference filters (FWHM of 1.5–10 nm) in order to reduce line blending which may occur due to the radiative decay of levels that are populated by state-to-state collision transfer.

The data acquisition equipment consists of two Boxcar integrator channels (Stanford Research Systems SR250) and a computer interface (Stanford Research Systems SR245), controlled by a LABVIEW program. A trigger generator (Stanford Research Systems DG535) has been used to control both the pump and dye lasers and to switch the sensitive gate of the photomultiplier. The time-resolved fluorescence measurements of the present investigations are acquired using a 1 GHz oscilloscope (Gagescope 82G).

For the analysis of the decay curves of the excited levels, the fluorescence signals from 900 and up to 2500 laser pulses have utilized. All the decay curves have been measured exactly at the center of the two-photon resonance which has first been redetermined in a spectral scan whenever the experimental conditions were changed. The background noise has been recorded and subtracted for all superposed data. From the background-corrected decay curve, the respective effective lifetime of a level at a given gas pressure was determined by a least-squares Levenberg-Marquardt fit to the sample data, taking into account the known instrumental response of the apparatus.

Unfortunately, an accurate determination of the laser power density thresholds for the amplified spontaneous emission (ASE) from the excited levels was not possible in our measurements. We assume that, for our excitation parameters, a possible occurrence of ASE is restricted to the excitation time during the temporal width of the laser pulse.

TABLE I. Measured and calculated lifetimes for the levels in neutral xenon discussed in this paper. λ_{exc} denotes the excitation wavelength and λ_{fl} denotes the wavelength of the observed fluorescence transition.

Level	Energy (cm^{-1})	λ_{exc} (nm)	λ_{fl} (nm)	Experimental values (ns)				Theoretical values (ns)		
				This work	Ref. [19]	Ref. [21]	Ref. [24]	This work	Ref. [19]	Ref. [21]
$8p[1/2]_0$	92555.135	2×216.1	407.8	207 ± 28		171 ± 9	212 ± 19	188.4		238.6
$5f[3/2]_2$	93366.245	2×214.2	747.2	94 ± 20	105 ± 6 [a]			114.3	91.3	
$5f[5/2]_2$	93403.966	2×214.1	745.1	78 ± 13	103 ± 7 [b]			95.6	98.6	

[a]The authors report a second value, 99 ± 6 ns, measured fluorescence at 394.8 nm.
[b]Measured fluorescence at 379.6 nm.

Therefore, we did not fit the data obtained during the first 10 ns counted from the fluorescence maximum when determining the effective lifetimes.

III. CALCULATION OF LIFETIMES

For excited levels, such as the $5f$, $6p$, $7p$, and $8p$ fine-structure states in atomic xenon, the MCDF method is known as versatile tool that often provides good-to-reliable theoretical predictions on the level energies, wave functions, oscillator strengths, and lifetimes [26,27]. For medium and heavy elements, in particular, this method enables one to account all the dominant relativistic and many-body effects on equal footings, including also the rearrangement of the bound electrons if the atom undergoes a transition. In the MCDF method [28], an atomic state is approximated by a linear combination of (so-called) configuration state functions (CSFs) of the same symmetry,

$$|\psi_\alpha(PJM)\rangle = \sum_{r=1}^{n_c} c_r(\alpha)|\gamma_r PJM\rangle, \tag{1}$$

where n_c is the number of CSFs and $\{c_r(\alpha)\}$ denotes the representation of the atomic state in the chosen basis. In most standard computations, the CSFs $|\gamma_r PJM\rangle$ are constructed as antisymmetrized products of a common set of orthonormal orbitals and are optimized together on the basis of the Dirac-Coulomb Hamiltonian. Relativistic effects due to the Breit interaction are then added to the representation $\{c_r(\alpha)\}$ by diagonalizing the Dirac-Coulomb-Breit Hamiltonian matrix [29,30]. Further quantum-electrodynamical corrections have been estimated but were found negligible for the excitation of a valence electron in atomic xenon.

For open-shell atoms, the main limitations in applying the MCDF model typically arise from missing parts in the electronic correlations due to the restricted size of wave function expansion (1). This limitation applies particularly if a quite large number of low-lying levels need to be generated altogether in order to compute the required transition probabilities and lifetimes. In the present lifetime computations, the atomic structure code GRASP92 [29] has been employed to generate the wave functions in a series of runs. Starting from the closed $5p^6\ ^1S_0$ ground level of xenon, two of the $5p$ electrons were allowed to be excited successively into the $6nl,7nl,\ldots$ subshells. In the largest expansion of the wave functions, finally single excitations up to the $9s$, $9p$, $8d$, and $7f$ orbitals were taken into account. A separate optimization was performed for the $5p^6\ ^1S_0$ ground levels as well as for the levels that have been measured experimentally in this paper (cf. Table I), namely, $5p^5 8p[1/2]_0$, and $5p^5 5f[3/2]_2$ and $5p^5 5f[5/2]_2$, respectively, while all other low-lying levels were obtained within an *extended-average-level* calculation in order to keep the computations feasible. By applying this computational procedure, excitation energies with an uncertainty of $\sim 1000\ cm^{-1}$ were obtained for all levels of interest. The proper selection of the (requested) levels out of those levels with the same symmetry J^P was tested in addition by analyzing the decomposition of the corresponding wave expansions in the symmetry adapted (jj as well as LS) basis [31].

From the wave functions, the transition probabilities and lifetimes were obtained by means of the REOS [32] component which is part of the RATIP program [33] for calculating a variety of (relativistic) atomic transition and ionization properties. Since the wave functions of the two-photon excited states were (re) optimized separately with regard to the lower-lying levels, parts of the orbital relaxation have been included also in this way into the transition probabilities. Owing to the rather high excitation of the $5p^5 8p[1/2]_0$, $5p^5 5f[3/2]_2$, and $5p^5 5f[5/2]_2$ levels from above (with several ten levels of different total angular momenta below of them), no attempt has been made to further monitor the convergence of the transition probabilities and lifetimes as the size of expansion (1) would be increased further. An additional test was made by comparing the results from different gauges in the radiation field for which an agreement within about 15% was obtained except for the lifetime of the $5p^5 8p[1/2]_0$ level.

IV. EXPERIMENTAL RESULTS AND DISCUSSION

To study the radiative lifetimes and collision kinetics in rare gases using TALIF spectroscopy, a standard procedure consists of the measurement of the transition rates at different pressures. The transition rates are hereby extracted from the observed time-resolved fluorescence signal, assuming a (single-component) exponential decay of the excited state. For the levels considered in this work, (rather) strong collisional deactivation occurs for all pressures down to ~ 5 Pa. From the pressure-dependent effective lifetime τ of the ex-

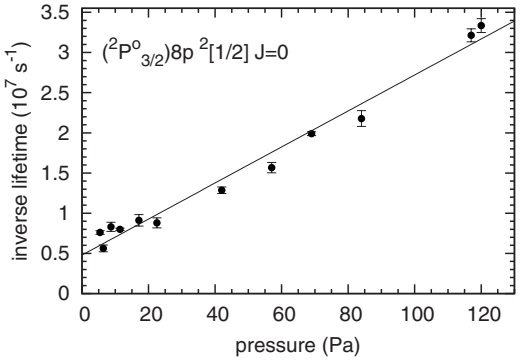

FIG. 2. Stern-Volmer plot of the decay rates for the $8p[1/2]_0$ level in neutral xenon.

cited levels, the spontaneous lifetime τ_0 then follows from the relation

$$\frac{1}{\tau} = \frac{1}{\tau_0} + Q, \tag{2}$$

where Q denotes the collisional deactivation rate. Since we consider here xenon atoms as the only quenching particle species, Q can be written in terms of the xenon particle density n,

$$Q = n\bar{v}\sigma, \tag{3}$$

with σ denoting the collisional cross section and $\bar{v}$ denoting the rms velocity of the xenon atoms. It is convenient to define the collisional deactivation coefficient $k_q = \bar{v}\sigma$. The spontaneous lifetime is extrapolated as the intercept of Eq. (2) at zero pressure, while the slope provides the deactivation coefficient (Stern-Volmer plot).

Within the Stern-Volmer method, consistent results have been obtained for the $5f[3/2]_2$, $5f[5/2]_2$, and $8p[1/2]_0$ levels. The xenon pressure has been varied between 4 and 120 Pa. In this pressure regime, influence of collisional deactivation on the effective lifetime has been found to be significant for all investigated levels. Results have been summarized in Table I.

The fluorescence decay of the $8p[1/2]_0$ level has been detected at 407.8 nm. The observed fluorescence line was isolated by using a band pass filter (central wavelength at 408.0 nm and bandwidth FWHM of 3.5 nm). No other lines of neutral xenon occur within the FWHM transmission interval of the filter [34]. A spontaneous lifetime of 207 ± 28 ns has been extracted from the Stern-Volmer plot (Fig. 2), in reasonable agreement within $\sim 10\%$ with our calculated value of 188.4 ns. The collisional deactivation coefficient for this level is $k_q = (9.0 \pm 0.5) \times 10^{-10}$ cm^3 s^{-1}. This is roughly a factor of 2 larger compared to the collisional deactivation coefficients found by Whitehead *et al.* [12] for the $7pJ = 0,2$ levels. Indeed, the measured effective lifetimes varied between 27 ns at 120 Pa and 166 ns at 6.6 Pa. Analyzing temporal fluorescence data at different pressures, we found no direct evidence for a multicomponent decay. This might be due to the (rather) distinct energetic separation of the

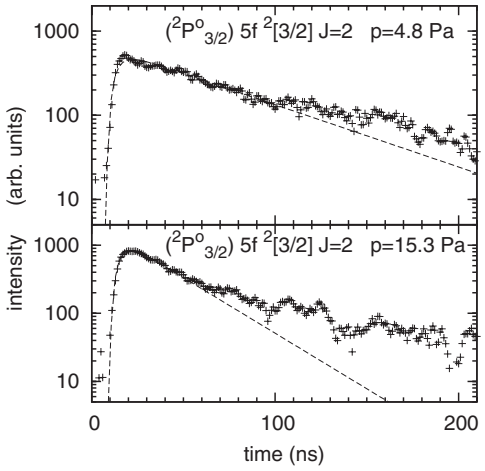

FIG. 3. Sample data of the time-resolved signal at 747.2 nm after excitation of the $5f[3/2]_2$ level at xenon pressures of 4.8 and 15.3 Pa. Besides a strong fast component, multicomponent character becomes visible.

$8p[1/2]_0$ level from its nearest neighbor $7d[7/2]_3$, which is about 91 cm^{-1}, and therefore quite large compared to splitting of the levels in the nf manifolds.

The situation is more complex for the $5f$ levels. The fluorescence after excitation of the $5f[3/2]_2$ level has been recorded at 747.2 nm using a band pass filter with central wavelength at 746.8 nm and a bandwidth FWHM of 3.4 nm. Figure 3 shows the typical temporal characteristics of the observed decays. At all pressures between 4.8 and 60 Pa, a strong fast component is present, while deviations from a single-exponential decay become visible after $\gtrsim 1.5\tau$. Note that Verdugo *et al.* [19] also observed a nonsingle-exponential decay of some nf levels and attributed this phenomenon to cascade contributions from higher excited levels. This assumption seems to be reasonable for electron-beam excitation experiments but would not be justified for the state-selective two-photon excitation as applied in our measurements. However, a line blending may possibly occur in the investigation of this level if collision transfer to the nearest neighbor levels (followed by radiative decay) is supposed to be a dominant process. For the transmission width of the given band pass filter, one further fluorescence line at 747.4 nm appears within the FWHM transmission width of the filter which belongs to the $5f[3/2]_1$ level. Both levels are separated from each other by only $\Delta E = 3.5$ cm^{-1}. However, because the splitting of the nf levels is very small in general, population of non-laser-excited levels through collisional transfer might affect a variety of states in the direct neighborhood. We are thus rather confident that there is no critical perturbation of our detected fluorescence signal due to line blending. Notice that the measurements carried out by Verdugo *et al.* [19] of this level also did not resolve the fine structure of the $5f$ levels in their detection apparatus completely. In addition, it is obvious that an electron-beam excitation mechanism cannot be as state selective as the narrow band two-photon excitation scheme used in the present setup.

Due to the close energetic spacing of the $5f$ and $9s$ levels, inverse collision transfer (leading to the repopulation of the laser-excited level) from neighbor states is most likely re-

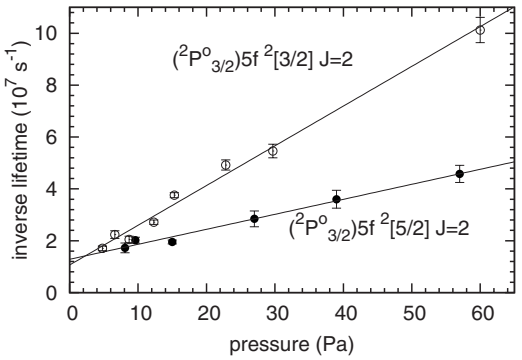

FIG. 4. Stern-Volmer plots of the decay rates (fast components) of $5f[3/2]_2$ and $5f[5/2]_2$.

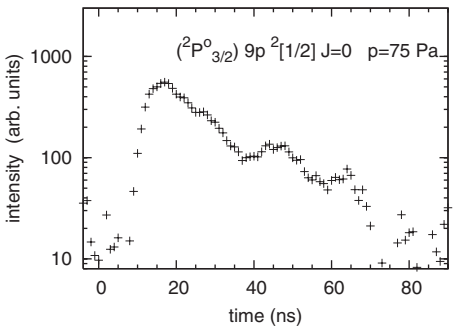

FIG. 5. Time-resolved signal of the $9p[1/2]_0$ level at xenon pressure of 75 Pa. The fluorescence was detected at 381.0 nm.

sponsible for multicomponent characteristics. A two-state coupled model under the assumption of detailed balance has been applied, e.g., by Bruce *et al.* [10], to find the state-to-state reaction rates from a two-component fluorescence decay. However, a detailed analysis of secondary components is very difficult to be carried out for our measured data since the signal-to-noise ratio does not allow us to resolve these components with sufficient accuracy. Furthermore, it is unknown how many levels need to be included finally in a coupled de-excitation scheme. To avoid an analysis in a too speculative manner, only the strong component is considered in the following. In Fig. 4, the strong fast component has been used to extrapolate the lifetime at zero pressure. Hereby, we have assumed that a linear dependency exists between the fast component decay constant and the xenon pressure within the investigated pressure range. If this approximation is correct, a spontaneous lifetime of 94 ± 20 ns is obtained from the extrapolation, in good agreement with the value given by Verdugo *et al.* [19], but is about 20% smaller than our computed value of 114.3 ns. For this level, the collisional deactivation coefficient is determined to be $k_q = (6.3 \pm 0.4) \times 10^{-9}$ cm^3 s^{-1}.

Fluorescence following the two-photon excitation of the $5f[5/2]_2$ level has been observed at 745.1 nm by using a band pass filter centered at 746.9 nm with a bandwidth FWHM of 4.5 nm. The Stern-Volmer plot is displayed in Fig. 4. For this fluorescence transition, a line blending could possibly arise from two lines at 747.4 and 747.2 nm that refer to the decay of the $5f[3/2]_1$ and $5f[3/2]_2$ levels, respectively. However, it appears not very probable that these lines to have influenced our measurements significantly. The spontaneous lifetime of 78 ± 13 ns is obtained, which is 20% lower than our theoretical estimate and even 25% lower than the value in [19]. These deviations may indicate a systematic underestimation of our effective lifetimes for the $5f$ levels due to the neglected influence of weaker, slower components in Fig. 3. The collisional deactivation coefficient is $k_q = (2.4 \pm 0.2) \times 10^{-9}$ cm^3 s^{-1}.

When compared with earlier measurements, we have assigned here relative large uncertainties of 15–20 % to the spontaneous lifetimes reported in this work. Most of the previous experiments were carried out at a pressures $<10^{-1}$ Pa, where the role of collisional deactivation is mostly negligible. Due to the limited sensitivity of our experiment, it was not possible to measure decay curves below 4 Pa with sufficient accuracy. However, this drawback is not too serious since the determination of two-photon absorption coefficients as well as two-photon calibration techniques can be performed at pressures for which the effective lifetime can be measured to a higher degree of accuracy. Furthermore, estimates of the collisional transition rates have been given here.

Further lifetime measurements have been performed also for two levels of the $6f$ and $9p$ terms. Fluorescence after two-photon excitation of $6f[5/2]_2$ level has been detected at 568.8 nm by using a band pass filter with transmission maximum at 568.2 nm and a FWHM bandwidth of 2.2 nm. Unfortunately, however, no clear enough signal could be obtained at pressures below 70 Pa to analyze the spontaneous lifetimes of these levels. On the basis of the spontaneous lifetime measured for this level by Verdugo *et al.* [19], our data indicate collisional deactivation rates of the same order as for the $5f[3/2]_2$ level. Comparing the three $9p$ configurations with $J=0,2$, a relative strong fluorescence signal has been detected after excitation of the $9p[1/2]_0$ resonance using a cutoff filter to prevent the detection of elastically scattered laser radiation. Thereafter, fluorescence of the $9p[1/2]_0$ level was isolated with a band pass filter with central wavelength at 380 and a FWHM bandwidth of 10 nm. Line blending may occur from $9p$ neighbor levels populated by collisions (the energetic separation is $\Delta E \geq 95$ cm^{-1}) and some $5f$ levels ($\Delta E \geq 865$ cm^{-1}). The decay curve of the isolated fluorescence at 381.0 nm at 75 Pa is shown in Fig. 5. The signal can be unambiguously identified; however, it shows distortions probably introduced by the data acquisition electronics due to the superposition of very weak signal intensities, which do not allow for a quantitative discussion of occurrence and influence of secondary components neither for reliable fits to the observed decay. An in-depth study of this level may be interesting for future investigations as no experimental lifetime data for the $9p$ levels is available.

V. CONCLUSION

A state-selective excitation has been achieved for some $8p$, $9p$, $5f$, and $6f$ levels in neutral xenon by applying two-photon excitation schemes. A quantitative analysis was made for levels of these multiplets with respect to radiative and

collisional transition rates using this technique. The spontaneous lifetimes have been extrapolated for $8p[1/2]_0$ and $5f[3/2]_2$, $5f[5/2]_2$ levels. Lifetimes for these levels have been calculated in the multiconfiguration Dirac-Fock method. The agreement between calculated and measured spontaneous lifetimes is 10–25 %. Significant collisional deactivation has been found at all pressures. The $5f$ states show multicomponent decay characteristics at pressures as low as 4–60 Pa. A detailed analysis of state-to-state interactions of these levels remains as the future work in order to allow for more sophisticated modeling of collision kinetics and implications on radiative transition rates. The results are important for the quantitative characterization of two-photon excitation schemes including these levels with regard to TALIF plasma diagnostics in xenon and for the development of two-photon reference schemes for the calibration of TALIF measurements in the spectral range around the respective two-photon transition wavelengths.

ACKNOWLEDGMENTS

C.E. wishes to thank the Evangelisches Studienwerk Villigst e.V. for financial and idealistic support through a Ph.D. scholarship. Authors gratefully acknowledge funding by the Deutsche Forschungsgemeinschaft (DFG) within Project No. Au85/24-1 and No. Fr 1251/13-2.

[1] A. C. Eckbreth, *Laser Diagnostic for Combustion Temperature and Species* (Abacus Press, Cambridge, MA, 1988).
[2] S. Löhle, C. Eichhorn, A. Steinbeck, S. Lein, G. Herdrich, H. P. Röser, and M. Auweter-Kurtz, Appl. Opt. **47**, 1837 (2008).
[3] D. Fletcher, Appl. Opt. **38**, 1850 (1999).
[4] A. Goehlich, T. Kawetzki, and H. F. Döbele, J. Chem. Phys. **108**, 9362 (1998).
[5] K. Niemi, V. Schulz-von der Gathen, and H. F. Döbele, J. Phys. D **34**, 2330 (2001).
[6] K. Niemi, V. Schulz-von der Gathen, and H. F. Döbele, Plasma Sources Sci. Technol. **14**, 375 (2005).
[7] J. K. Ku and D. W. Setser, J. Chem. Phys. **84**, 4304 (1986).
[8] N. Böwering, M. R. Bruce, and J. W. Keto, J. Chem. Phys. **84**, 709 (1986).
[9] N. Böwering, M. R. Bruce, and J. W. Keto, J. Chem. Phys. **84**, 715 (1986).
[10] M. R. Bruce, W. B. Layne, C. A. Whitehead, and J. W. Keto, J. Chem. Phys. **92**, 2917 (1990).
[11] W. L. Alford, J. Chem. Phys. **96**, 4330 (1992).
[12] C. A. Whitehead, H. Pournasr, M. R. Bruce, Hong Cai, J. Kohel, W. B. Layne, and J. W. Keto, J. Chem. Phys. **102**, 1965 (1995).
[13] H. F. Döbele, T. Mosbach, K. Niemi, and V. Schulz-von der Gathen, Plasma Sources Sci. Technol. **14**, S31 (2005).
[14] S. Kröll and W. K. Bischel, Phys. Rev. A **41**, 1340 (1990).
[15] W. Gornik, S. Kindt, E. Matthias, and D. Schmidt, J. Chem. Phys. **75**, 68 (1981).
[16] T. D. Raymond, N. Böwering, C.-Y. Kuo, and J. W. Keto, Phys. Rev. A **29**, 721 (1984).
[17] C. H. Chen, G. S. Hurst, and M. G. Payne, Chem. Phys. Lett. **75**, 473 (1980).
[18] J. C. Miller, Phys. Rev. A **40**, 6969 (1989).
[19] D. Verdugo, M. Shaw, and J. Campos, Physica B & C **141**, 329 (1986).
[20] M. B. Das and S. Karmakar, Eur. Phys. J. D **32**, 285 (2005).
[21] E. Jiménez, J. Campos, and C. Sánchez del Río, J. Opt. Soc. Am. **64**, 1009 (1974).
[22] L. Allen, D. G. C. Jones, and D. G. Schofield, J. Opt. Soc. Am. **59**, 842 (1969).
[23] M. Chenevier and T. D. Nguyen, Phys. Lett. **36A**, 177 (1971).
[24] Ya. F. Verolainen and A. L. Osherovich, Opt. Spectrosc. **27**, 14 (1969).
[25] G. Racah, Phys. Rev. **61**, 537 (1942).
[26] C. Z. Dong, S. Fritzsche, B. Fricke, and W.-D. Sepp, Mon. Not. R. Astron. Soc. **307**, 809 (1999).
[27] S. Fritzsche, C. Z. Dong, and E. Träbert, Mon. Not. R. Astron. Soc. **318**, 263 (2000).
[28] I. P. Grant, in *Methods in Computational Chemistry*, edited by S. Wilson (Plenum Press, New York, 1988), Vol. 2, p. 1.
[29] F. A. Parpia, C. Froese Fischer, and I. P. Grant, Comput. Phys. Commun. **94**, 249 (1996).
[30] S. Fritzsche, C. Froese Fischer, and G. Gaigalas, Comput. Phys. Commun. **148**, 103 (2002).
[31] G. Gaigalas, T. Zalandauskas, and S. Fritzsche, Comput. Phys. Commun. **157**, 239 (2004).
[32] S. Fritzsche, C. Froese Fischer, and C. Z. Dong, Comput. Phys. Commun. **124**, 340 (2000).
[33] S. Fritzsche, J. Electron Spectrosc. Relat. Phenom. **114-116**, 1155 (2001).
[34] E. B. Saloman, J. Phys. Chem. Ref. Data **33**, 765 (2004).